ISBN 82–553–0705–2
Applied Mathematics

No 3
June 1990

Instability of Buckley-Leverett flow in heterogeneous media

by

Hans Petter Langtangen*,
Aslak Tveito**, Ragnar Winther**

PREPRINT SERIES – Matematisk institutt, Universitetet i Oslo

*Department of Mathematics, University of Oslo, P.O.Box 1053
** Department of Informatics, University of Oslo, P.O.Box 1080

Instability of Buckley-Leverett Flow in Heterogeneous Media

Hans Petter Langtangen* Aslak Tveito** Ragnar Winther**

June 24, 1990

Abstract

We study the simultaneous uni–directional flow of water and oil in a heterogeneous medium modelled by the Buckley–Leverett equation. It is shown both by analytical solutions and by numerical experiments that this hyperbolic model is unstable in the following sense: Perturbations in physical parameters in a tiny region of the reservoir may lead to a totally different picture of the flow. This means that simulation results obtained by solving the hyperbolic Buckley–Leverett equation are unreliable.

*Department of Mathematics, University of Oslo, P.O. Box 1053, 0316 Oslo 3, Norway

** Department of Informatics, University of Oslo, P.O. Box 1080, 0316 Oslo 3, Norway.

This research has been supported by VISTA, a research cooperation between the Norwegian Academy of Science and Letters and Den norske stats oljeselskap a.s. (Statoil).

Symbols and notation

x^*	spatial coordinate
L^*	characteristic length
x	dimensionless spatial coordinate
t^*	time coordinate
t_c^*	characteristic time
t	dimensionless time coordinate
s	water saturation
v^*	total filtration (Darcy) velocity
f	fractional flow function varying with s and x
ψ^*	diffusion function varying with s and x^*
ψ	dimensionless diffusion function varying with s and x
P_c^*	capillary pressure function
p_c^*	characteristic pressure
P_c	dimensionless capillary pressure function
ϕ	porosity
k^*	absolute permeability
k_c^*	characteristic absolute permeability
k	dimensionless absolute permeability
k_{rw}	relative water permeability
k_{ro}	relative oil permeability
μ_w^*	dynamic water viscosity
μ_o^*	dynamic oil viscosity
μ_c^*	characteristic viscosity

μ_w	dimensionless dynamic water viscosity
μ_o	dimensionless dynamic oil viscosity
ϱ_w^*	density of water
ϱ_o^*	density of oil
ϱ_c^*	characteristic density
ϱ_w	dimensionless density of water
ϱ_o	dimensionless density of oil
g	acceleration due to gravity
α	angle between flow direction and horizontal direction
W, β, v	dimensionless numbers defined by equations (4), (5) and (6)
ϵ	parameter measuring the capillary effects
I_δ	interval containing a low permeable rock
δ	length of I_δ
$\tilde{x}$	centroid of I_δ
$\bar{f}$	value of f outside I_δ
$\hat{f}$	value of f inside I_δ
s_δ	s for a fixed value of δ in section 3
S_1, S_2, S_3	constant values of s
σ_1, σ_2, σ	shock speeds
T	value of t
Δx	spatial grid spacing
Δt	temporal grid spacing
x_j	spatial grid point, $x_j = j\Delta x$
t_n	temporal grid point, $t_n = n\Delta t$
S_j^n	numerical approximation to $s(x_j, t_n)$
f_j^n	value of f at S_j^n and x_j

ψ_j^n	value of ψ at S_j^n and x_j
$\bar{x}(t)$	discontinuity curve in (x,t) space
$\bar{x}+$	right limiting value of $\bar{x}$
$\bar{x}-$	left limiting value of $\bar{x}$
s^L	left state of s (wrt. $\bar{x}$)
s^R	right state of s (wrt. $\bar{x}$)
$\tilde{f}$	local approximation of f around $\bar{x}$
f^-, f^+	values of $\tilde{f}$
$\bar{s}$	value of s at $\bar{x}$
S	similarity solution
ζ	argument of S
L^1	the space of absolutely integrable functions
L^∞	the space of bounded functions

1 Introduction

An important application of mathematical models for two–phase porous media flow in reservoir engineering is the simulation of waterflooding, that is, displacement of oil in an oil reservoir by injected water. Most of the mathematical theory for water flooding models, including stability properties, has been developed under the assumption of a homogeneous or a smoothly varying heterogeneous medium. Our purpose with this paper is to demonstrate that a certain instability phenomenon may arise when these models are applied for discontinuous heterogeneous media and capillary pressure effects are neglected.

Let us consider two–phase flow of water and oil in a porous medium. If the flow is one–dimensional, both phases are incompressible and if the volumetric flow rate is known, the saturation of the water phase $s(x,t)$, at position x and time t, is governed by the following (dimensionless) equation:

$$\phi\frac{\partial s}{\partial t}+v\frac{\partial f}{\partial x}=\frac{\partial}{\partial x}\left(\varepsilon\psi\frac{\partial s}{\partial x}\right). \tag{1}$$

Here ϕ is the porosity, v is the (scaled) volumetric total flow rate, f is the fractional flow function, and $\varepsilon\psi$ is related to capillary pressure effects. Both f and ψ are functions of s, and if the medium is heterogeneous they may also depend explicitly on x. In the latter case ϕ may also be a function of x. Equation (1) is derived from the principle of mass conservation for each phase, Darcy's law with relative permeabilities for each phase and the assumption of incompressible phases. The particular scaling used to derive (1) is described in Section 2. The one–dimensional flow equation (1) is commonly used as a simple tool for understanding the important performance properties of waterflooding.

For many reservoir engineering purposes the capillary effects are quite small, and the diffusion term in (1) is often neglected. In such cases s is governed by the Buckley–Leverett equation

$$\phi\frac{\partial s}{\partial t}+v\frac{\partial f}{\partial x}=0. \tag{2}$$

The Buckley–Leverett equation is an example of a hyperbolic conservation law for which a rigorous mathematical theory exists. It is an essential part of the Buckley-Leverett theory that for each x the function f is a nonlinear function of s. In most applications f is considered to be an "s-shaped" function of s. In the present paper we shall primary be interested in effects that occur due to the spatial variation of the fractional flow function

f. This variation will occur e.g. if the absolute permeability of the medium depends on x.

The Buckley–Leverett equation is usually studied as an initial value problem with a given initial saturation $s(x,0)$. It is well known that the solutions of nonlinear conservation laws of the form (2) can develop discontinuities. Hence, in order to obtain global solutions in time, we have to allow discontinuous weak solutions of the differential equation (2). Furthermore, extra entropy conditions for the discontinuities have to be added to the model in order to pick the physical solution. The proper discontinuities, which satisfy the entropy condition, will be referred to as shock waves. We will describe these well-known properties of scalar conservation laws more detailed in Section 5.

If the fractional flow function f varies smoothly with x, the properties of the entropy-solutions of equations of the form (2) are well understood. For example, stability (in the L^1–norm) with respect to perturbations in the initial data is established by Kruzkov (1970), and stability with respect to perturbations in the fractional flow function is discussed by Lucier (1985). However, if f is allowed to be a discontinuous function of x then most of the established theory for scalar conservation laws does not apply. In particular, there seems to be no result in the literature which confirms that the solution depends continuously on the fractional flow function in this case. Since discontinuous media are frequently encountered in reservoir modelling, and since the fractional flow function only can be specified with limited accuracy, this seems to be an essential question for the application of the Buckley-Leverett theory to heterogeneous media. We mention that Riemann problems for scalar conservation laws with discontinuous flux functions are discussed by Gimse and Risebro (1990).

The purpose of this paper is to investigate the properties of (2) in regimes where the fractional flow function f is a discontinuous function of x, by numerical experiments. In particular, we are concerned with the dependence of the solution on the fractional flow function. Our experiments show that small perturbations in the fractional flow function may lead to large perturbations in the solutions. Hence, in this sense the Buckley-Leverett equation is not a well-posed problem in these regimes.

In our calculations we have used piecewise constant fractional flow functions (as functions of x). This corresponds to a layered porous medium. If the initial data also are piecewise constant with respect to x, the solution of the initial value problem will, at least

for a short time, correspond to solutions of several Riemann problems. In fact, our examples of noncontinuous dependence will typically be constructed by considering situations which correspond to two noninteracting Riemann problems.

It seems that the instability property for the model (2) is only present when both positive and negative characteristic speeds are allowed. Physically this corresponds to a nonhorizontal reservoir where gravitational effects are significant. In some sense the instability observed for the model (2) is closely related to similar properties for non-strictly hyperbolic 2×2 systems (cf. e.g. Isaacson and Temple, and Tveito and Winther, 1990).

In order to obtain a better understanding of the instability phenomenon described above, we will compare the results obtained by the Buckley-Leverett equation (2) with results obtained by model (1) which includes diffusion effects. We will study both a nonlinear physical diffusion, generated by the capillary pressure, as well as a linear counterpart where ψ is considered constant.

The results of the numerical experiments with the convection diffusion models show that the continuous dependence of the solution with respect to the fractional flow function is regained when a diffusion term is included in the model. Hence, our experiments seems to indicate that, in regimes where the fractional flow function is allowed to be a discontinuous function of x, the hyperbolic Buckley-Leverett equation is not a satisfactory model. In contrast to the homogeneous case, a diffusion term has to be included in order to obtain a well-behaved model.

In Section 2 we present the different mathematical models to be considered and the relations between them. In Section 3 we discuss some analytical solutions of (2). This discussion is the main motivation for the experiments presented in Section 4. Some theoretical questions which arise from the results of our computations are considered in Section 5. In particular, we discuss viscous profiles associated to the shock waves of (2) when the shock coincide with a discontinuity in the fractional flow function. The results of this discussion will be used in order to explain the effects observed in our calculations. Finally, our conclusions are given in Section 6.

2 The mathematical models

The purpose of this section is to give a brief review of the different mathematical models to be used in our experiments. For a more detailed introduction to this material we refer to e.g. Aziz and Settari (1979).

Let x^* and t^* be the physical space and time coordinate, respectively. From the principle of mass conservation of each fluid phase, Darcy's law with relative permeabilities for each fluid phase, the assumption of incompressible phases and one–dimensional flow, the following equation for the water saturation $s(x^*, t^*)$ can be derived:

$$\phi \frac{\partial s}{\partial t^*} + v^* \frac{\partial f}{\partial x^*} = -\frac{\partial}{\partial x^*}\left(\psi^* \frac{dP_c^*}{ds}\frac{\partial s}{\partial x^*}\right), \quad 0 < x^* < L^*, \tag{3}$$

where $L^* > 0$ is the total length of the reservoir. Furthermore, ϕ denotes the porosity of the medium. In a heterogeneous medium ϕ may be a function of the spatial variable x^*. The variable v^* is the total filtration velocity. Throughout the paper we assume that v^* is constant in time. Note that v^* is independent of x^* in one–dimensional flow of incompressible phases. If v^* is known, equation (3) determines $s(x^*, t^*)$.

The fractional flow function f is in general a function of s and x^*. It is given by the expression

$$f = \frac{k_{rw}[\mu_w^*]^{-1} + k^* k_{rw} k_{ro}[\mu_w^* \mu_o^* v^*]^{-1}(\varrho_w^* - \varrho_o^*) g \sin\alpha}{k_{rw}[\mu_w^*]^{-1} + k_{ro}[\mu_o^*]^{-1}}.$$

The densities of water and oil, denoted by ϱ_w^* and ϱ_o^* respectively, are assumed to be constants. Similarly, the constants μ_w^* and μ_o^* denote the corresponding (dynamic) viscosities. Furthermore, g is the acceleration due to gravity and the constant α denotes the dip angle of the reservoir. The absolute permeability is denoted by k^*. The relative permeabilities, k_{rw} and k_{ro}, are functions of s, while, in a heterogeneous medium, the relative permeabilities and the absolute permeability may also depend explicitly on x^*.

The diffusion function ψ^* is given by

$$\psi^* = \frac{k^* k_{rw}[\mu_w^*]^{-1} k_{ro}[\mu_o^*]^{-1}}{k_{rw}[\mu_w^*]^{-1} + k_{ro}[\mu_o^*]^{-1}}.$$

It follows that ψ^* is in general a function of s and x^*.

Finally, P_c^* denotes the capillary pressure and is a nonincreasing function of s. In a heterogeneous medium P_c^* may also vary with x^*. Throughout the paper we will assume for simplicity that dP_c^*/ds is a nonpositive constant.

In order to transform the equation (3) into dimensionless form we introduce characteristic quantities for time, absolute permeability, viscosity, density and pressure denoted by $t_c^*, k_c^*, \mu_c^*, \varrho_c^*$ and p_c^*, respectively. Recall that s and ϕ are dimensionless by their definition. New dimensionless quantities (without asterix) are then defined as

$$\begin{aligned} x &= x^*/L^* \\ t &= t^*/t_c^* \\ k &= k^*/k_c^* \\ \mu_w &= \mu_w^*/\mu_c^* \\ \mu_o &= \mu_o^*/\mu_c^* \\ \varrho_w &= \varrho_w^*/\varrho_c^* \\ \varrho_o &= \varrho_o^*/\varrho_c^* \\ P_c &= P_c^*/p_c^* \end{aligned}$$

Furthermore, we let the nonnegative constant ε be given by $\varepsilon = -W(dP_c/ds)$, where W is a dimensionless number

$$W = \frac{p_c^* t_c^* k_c^*}{(L^*)^2 \mu_c^*}. \tag{4}$$

The dimensionless diffusion function ψ now becomes

$$\psi = \frac{k k_{rw}/\mu_w \cdot k_{ro}/\mu_o}{k_{rw}/\mu_w + k_{ro}/\mu_o}.$$

If we introduce the dimensionless numbers v and β, given as

$$v = \frac{t_c^* v^*}{L^*} \tag{5}$$

$$\beta = \frac{\varrho_c^* k_c^* g \sin\alpha}{\mu_c^* v^*}, \tag{6}$$

the scaled fractional flow function f can be expressed as

$$f = \frac{k_{rw}/\mu_w + \beta k k_{rw} k_{ro} [\mu_w \mu_o]^{-1} (\varrho_w - \varrho_o)}{k_{rw}/\mu_w + k_{ro}/\mu_o}. \tag{7}$$

The governing equation (3) now takes the form

$$\phi \frac{\partial s}{\partial t} + v \frac{\partial f}{\partial x} = \varepsilon \frac{\partial}{\partial x}\left(\psi \frac{\partial s}{\partial x}\right), \quad 0 < x < 1. \tag{8}$$

We recall that f and ψ are in general nonlinear functions of s and x and that the diffusion coefficient ψ is nonnegative. If $\psi > 0$ the model (8) is a parabolic differential equation. Furthermore, since ε usually is small, the equation is a convection dominated diffusion equation. If the diffusion term on the right hand side of (8) is neglected, we obtain the hyperbolic Buckley-Leverett equation

$$\phi \frac{\partial s}{\partial t} + v \frac{\partial f}{\partial x} = 0, \quad 0 < x < 1. \tag{9}$$

In our numerical experiments we shall investigate the properties of the two models (8) and (9). In addition we will also consider a model with linear diffusion, that is, the equation (8) with ψ chosen to be a constant.

3 An example of instability

Our aim with this section is to present an example which shows that the solution of the Buckley-Leverett equation (9) is very sensitive with respect to certain perturbations in the fractional flow function. A perturbation of the fractional flow function on a very small spatial interval, for example due to a low permeable thin rock layer, may lead to a large perturbation in the solution. This example clearly reduces the reliability of simulation results based on hyperbolic models for two-phase flow.

The qualitative behaviour of the Buckley–Leverett equation is not affected by the numerical values of the constants ϕ and v. For simplicity we therefore set these constants equal to unity. Consider then the Buckley-Leverett equation (9) with a fractional flow function on the form

$$f(s,x) = \begin{cases} \bar{f}(s) & \text{if } x \notin I_\delta, \\ \hat{f}(s) & \text{if } x \in I_\delta. \end{cases}$$

Here $I_\delta = (\tilde{x} - \delta/2, \tilde{x} + \delta/2)$, and $\bar{f}$ and $\hat{f}$ are fractional flow functions corresponding to different values of the absolute permeability, cf. (7). The interval I_δ is a low permeable region. Inside I_δ the absolute permeability function is small, and outside I_δ the absolute permeability is large. In the next section we will give precise data for this situation to be used in the numerical experiments. In Figure 1 we have sketched $\bar{f}$ and $\hat{f}$.

Let S_1 denote the point at which the upper fractional flow function, $\hat{f}$, takes on it minimum, cf. Figure 1. We consider the pure initial value problem for the Buckley-Leverett

equation with the initial data

$$s(x,0) = S_1.$$

Let $s_\delta = s_\delta(x,t)$ denote the solution of this problem for a fixed value of δ. We observe that in the case of $\delta = 0$, the solution of the problem is trivial,

$$s_0(x,t) = S_1.$$

In the case of $\delta > 0$ the initial value problem consists of two Riemann problems. We refer to Allen, Behie and Trangenstein (1988) for an introduction to Riemann problems for the Buckley-Leverett equation. We will return to the discussion of such problems in Section 5. Here we will merely observe that the initial value problem stated above consists of two exact solvable Riemann problems. The first Riemann problem, situated at $x = \tilde{x} - \delta/2$, has the left state S_1 and the left flux function $\bar{f}$. The right state is also S_1, but the right flux function is $\hat{f}$. The solution of this problem consists of a shock from S_1 to a state S_2 with a negative shock speed σ_1, followed by a shock from S_2 back to S_1 with the shock speed equal to zero. The state S_2 satisfies $\bar{f}(S_2) = \hat{f}(S_1)$ and $S_2 < S_1$.

In the next Riemann problem, located at $x = \tilde{x} + \delta/2$, the left and right state are still S_1, but now the left flux function is $\hat{f}$ and the right flux function is $\bar{f}$. The solution of this problem is composed of a shock of zero speed from S_1 to S_3, where S_3 satisfies $\hat{f}(S_1) = \bar{f}(S_3)$ and $S_1 < S_3$, followed by a shock with positive speed σ_2 from S_3 back to S_1.

In Figure 1 the solutions of the two Riemann problems are graphed in the (s,f) space, and in Figure 2 the solutions are shown in the (x,t) space.

As we mentioned above, the solution of the problem with $\delta = 0$ consists only of the constant state S_1. Consider the solution of the initial value problem with $\delta > 0$ at some fixed time $T > 0$. In order for this problem to be stable with respect to perturbations in the fractional flow function, the solution $s_\delta(\cdot,T)$ must converge towards $s_0(\cdot,T) = S_1$ as δ tends to zero. From Figure 2, we clearly see that this is not the case. In fact, as δ tends to zero, s_δ converge towards a function of the form depicted in Figure 3.

We have observed that, according to the hyperbolic Buckley-Leverett equation, a change in the value of the absolute permeability function in a tiny region in the reservoir totally changes the behaviour of the flow. This means that in order to simulate the displacement of oil by water in a heterogeneous medium, the values of the absolute permeability function

have to be known to an extreme degree of accuracy in order to get reliable results, since small uncertainties in this functions produces large uncertainties in the solutions. Now, it is of course impossible to obtain the absolute permeability function, or any other of the physical data involved, to such a degree of accuracy. We therefore have to conclude that the Buckley-Leverett model of two phase flow in a heterogeneous medium may produce erroneous predictions of the oil recovery.

Fortunately, the numerical experiments reported in the next section indicate that well-posedness is restored when a diffusion term is taken into account.

From a mathematical point of view, it is interesting to note that the hyperbolic problem may be stable in a suitable pair of norms. We have observed that small perturbations measured in the L^1-norm (with respect to x) of the fractional flow function may lead to large perturbations in the L^1-norm of the solution. However, we believe that the perturbations of the solutions measured in L^1 may be bounded by a stronger norm on the perturbations of the fractional flow function, say the $L^\infty-$norm. Such a stability results has, however, limited practical interest since, due to the heterogeneous medium, the uncertanties of the fractional flow function is very large in such a strong norm.

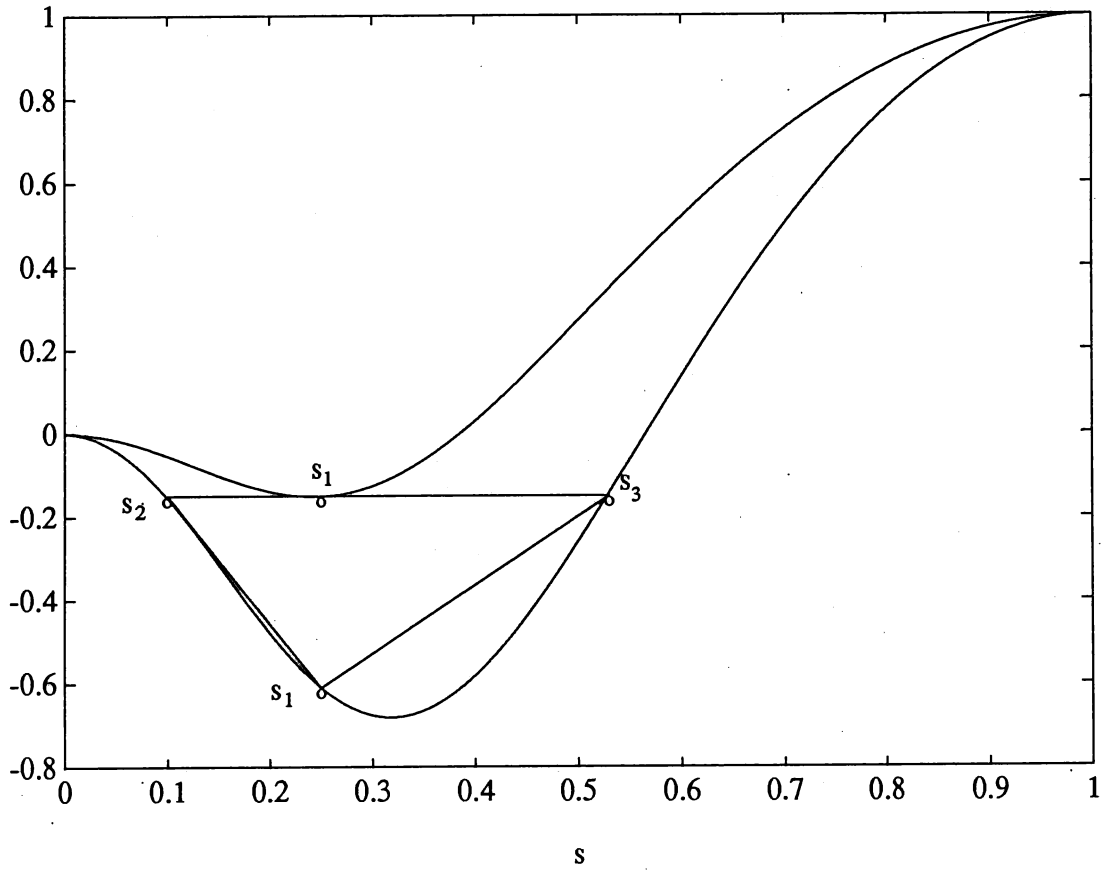

Figure 1: *Solution of the initial value problem in the* (s, f) *space. The lower curve is* $\bar{f}$ *and the upper curve is* $\hat{f}$.

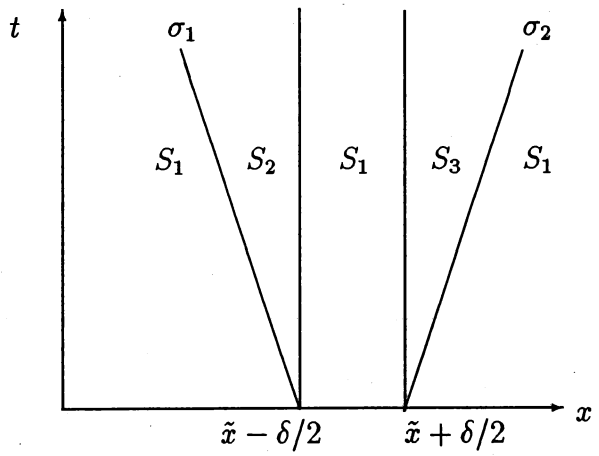

Figure 2: *The solution of the initial value problem in the (x,t) space. Note that the waves of the two Riemann problems are non-interacting for all $\delta > 0$ and $t > 0$.*

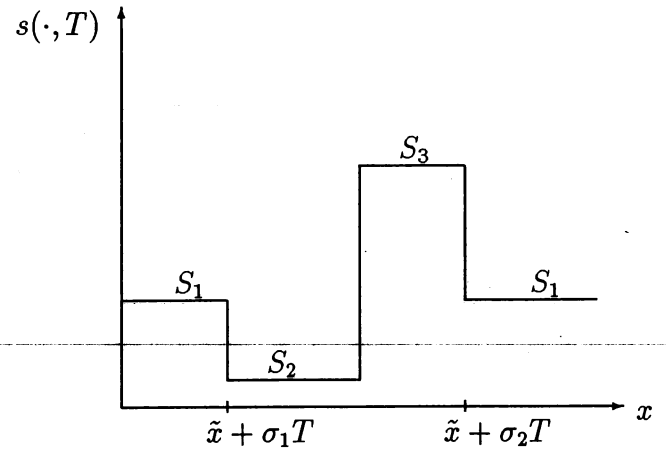

Figure 3: *The limit of $s_\delta(\cdot, T)$ as δ goes to zero. Recall that $\sigma_1 < 0$ and $\sigma_2 > 0$.*

4 Numerical Experiments

In this section we will present a computational study of the stability for the parabolic problem (8) and the hyperbolic problem (9). A standard numerical scheme will be used to generate approximate solutions of the initial value problems of the kind that were studied in the previous section. For the hyperbolic model (9) the explicit Lax-Friedrichs scheme is used, while, in order to avoid stability problems, we have chosen to use an implicit scheme for the parabolic model (8). The convergence of these schemes are rather slow, but since we are dealing with one–dimensional problems we can afford to use a rather fine mesh. On the other hand, the advantage of the schemes is that both theory and experience seem to indicate that they always will converge to the proper solution when they are applied to the problems under consideration here. Hence, by using a sufficiently fine mesh, we can expect to compute the desired solutions sufficiently accurately.

Let $\Delta t > 0$ denote the time step and Δx the spatial grid size. The grid points are then defined by $(x_j, t_n) = (j\Delta x, n\Delta t)$. We will let S_j^n denote the approximations of the saturation s at the grid points, that is, $S_j^n \approx s(x_j, t_n)$. Similarly, we let $f_j^n = f(S_j^n, x_j)$. The parabolic equation (8) is now approximated by the difference scheme

$$\phi\frac{S_j^{n+1} - S_j^n}{\Delta t} + v\frac{f_{j+1}^{n+1} - f_{j-1}^{n+1}}{2\Delta x} = \varepsilon\left(\frac{\psi_{j+1/2}^{n+1}(S_{j+1}^{n+1} - S_j^{n+1}) - \psi_{j-1/2}^{n+1}(S_j^{n+1} - S_{j-1}^{n+1})}{(\Delta x)^2}\right), \quad (10)$$

where $\psi_{j+1/2}^{n+1} = \frac{1}{2}(\psi(S_j^{n+1}, x_j) + \psi(S_{j+1}^{n+1}, x_{j+1}))$. This scheme requires the solution of a nonlinear system of algebraic equations for each time step. These systems are solved by a standard fixed point iteration.

The explicit Lax-Friedrichs scheme for the hyperbolic equation (9) takes the form

$$\phi\frac{S_j^{n+1} - \frac{1}{2}(S_{j+1}^n + S_{j-1}^n)}{\Delta t} + v\frac{f_{j+1}^n - f_{j-1}^n}{2\Delta x} = 0. \quad (11)$$

We consider the same initial value problem as we described in the previous section with $\tilde{x} = 0.3$. The absolute permeability function has one value inside the interval $I_\delta = (\tilde{x} - \delta/2, \tilde{x} + \delta/2)$, and another value outside the interval. In the numerical experiments we have used the following physical parameters: $L^* = 625$ m, $t_c^* = 8.64 \cdot 10^7$ s (1000 days), $k_c^* = 5 \cdot 10^{-13}$ m^2 (appr. 500 md), $\mu_c^* = 10^{-4}$ kg/ms, $\varrho_c^* = 10^3$ kg/m^3, $g = 9.81$ m/s^2, and $v^* = 1.74 \cdot 10^{-6}$ m/s. Values of the dimensionless parameters were $\varrho_w - \varrho_o = 0.1$, $\mu_o = 4$,

$\mu_w = 1$, $\sin\alpha = -0.5$, $\phi = 0.24$, $k_{rw} = s^2$, and $k_{ro} = (1-s)^2$. This implies $v = 0.24$ and $\beta = -14.13$. The absolute permeability function $k(x)$ was chosen equal to 15 outside I_δ and equal to 7.5 inside this interval.

With these parameters we obtain the following equation

$$\frac{\partial s}{\partial t} + \frac{\partial f}{\partial x} = \epsilon \frac{\partial}{\partial x}\left(\psi \frac{\partial s}{\partial x}\right),$$

where the fractional flow function is given by

$$f(s,x) = \frac{s^2 - 0.3533k(x)s^2(1-s)^2}{s^2 + \frac{1}{4}(1-s)^2}$$

and the diffusion function is given by

$$\psi(s,x) = 0.4608\frac{k(x)s^2(1-s)^2}{(1-s)^2 + 4s^2}.$$

This fractional flow function is graphed for two values of x in Figure 1. For these parameters, the minimum of the upper fractional flow function is attained at about $S_1 = 0.25$.

We also consider the case of a linear diffusion term. This is achieved by approximating the diffusion function ψ by the constant value $\bar{\psi} = \psi(S_1, 0)$.

We generate numerical solutions of the equation for $(x,t) \in (0,1)\times(0,0.01]$ with several values of ϵ and δ. We have used the mesh parameters $\Delta x = 1/2000$ and $\Delta t = 0.01/2000$, and the initial condition

$$s(x,0) = S_1 = 0.25 \quad \forall x \in (0,1).$$

In Figure 4 the numerical solutions at $t = 0.01$ of the initial value problem for $\epsilon = 0.5$ is presented for several values of δ. We observe that the solution tends towards the constant state $S_1 = 0.25$ as δ tends to zero. We also observe that the solution of the problem with linear diffusion is fairly close to the solution of the problem with nonlinear diffusion for all δ. In Figure 5, the corresponding solutions are given for $\epsilon = 0.1$. Again the solutions converges towards the constant state S_1 as δ tends to zero, but the convergence is slower. In Figure 6 we have used $\epsilon = 0.01$, i.e. the problem is almost hyperbolic, and we observe that the solutions seems to converge towards a certain nonconstant profile as δ tends to zero. Finally, in Figure 7 the numerical solution of the hyperbolic problem is given. We observe, again, that the solution of this problem tends toward a profile different from the

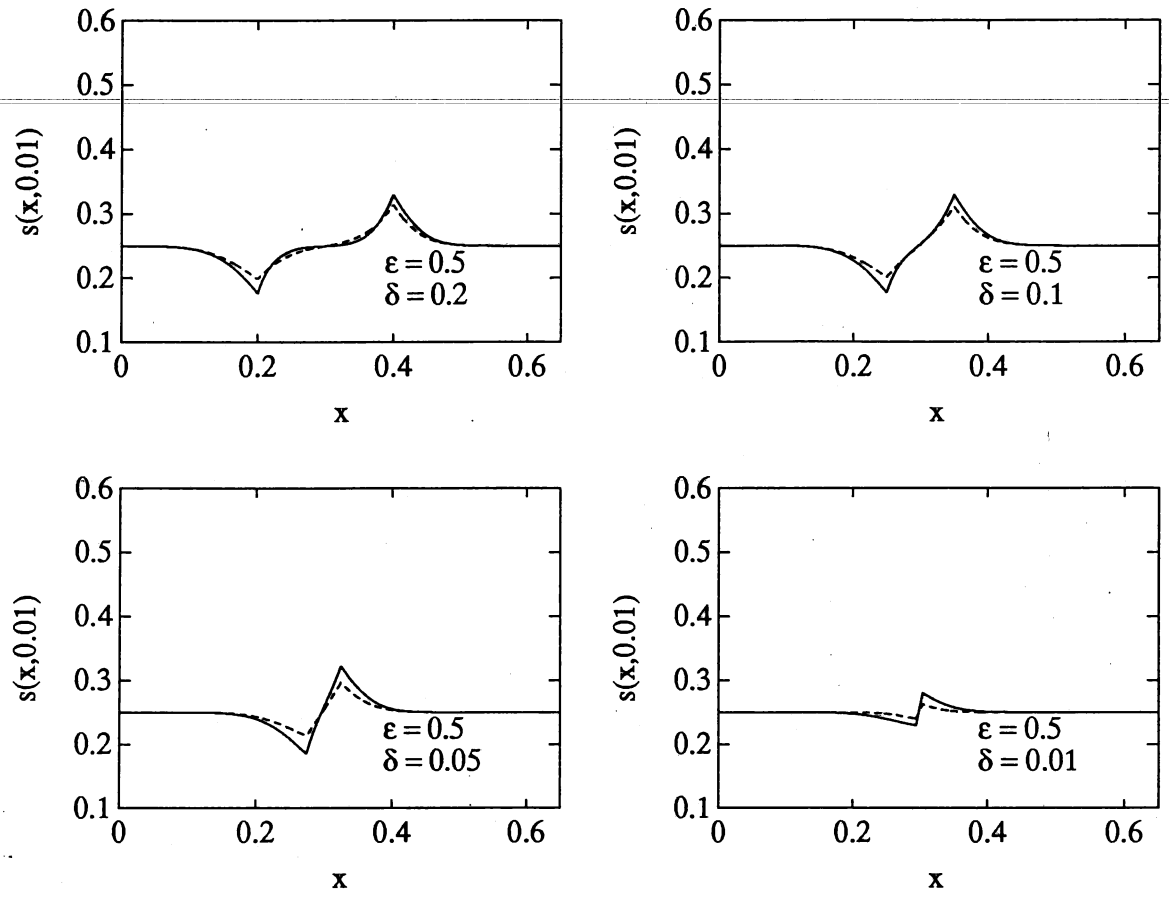

Figure 4: *The numerical solution of the initial value problem for a fixed $\varepsilon = 0.5$ with four different values of δ. Solid line: non-linear diffusion, dotted line: linear diffusion.*

constant state as δ tends to zero. This experiment verifies the observations presented in the previous section.

We have seen, both numerically and analytically, that the hyperbolic Buckley-Leverett equation is very sensitive to changes in the fractional flow function on small spatial intervals. Our computational study clearly indicates that if a certain amount of diffusion is taken into account, well posedness is regained. In fact, the experiments indicate that the stability of the problem increases with increasing values of ε.

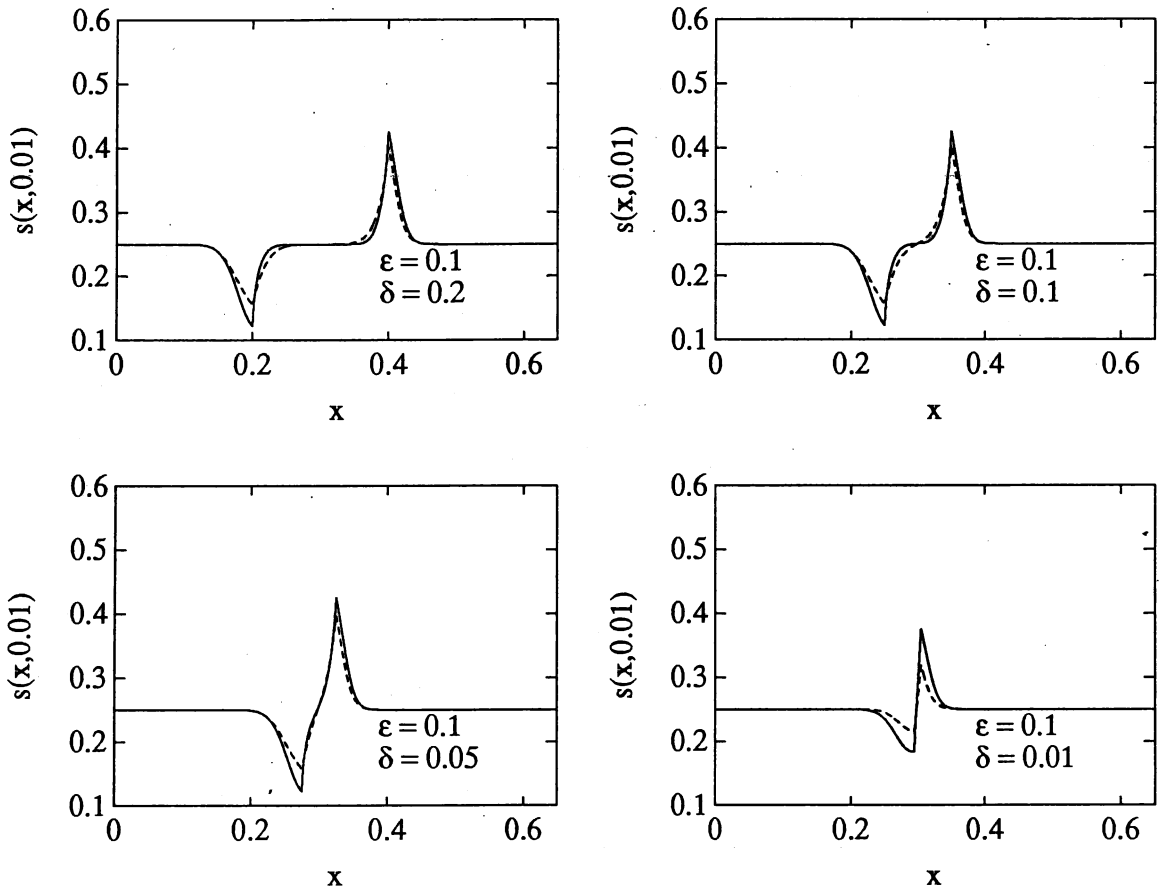

Figure 5: *The numerical solution of the initial value problem for a fixed $\varepsilon = 0.1$ with four different values of δ. Solid line: non-linear diffusion, dotted line: linear diffusion.*

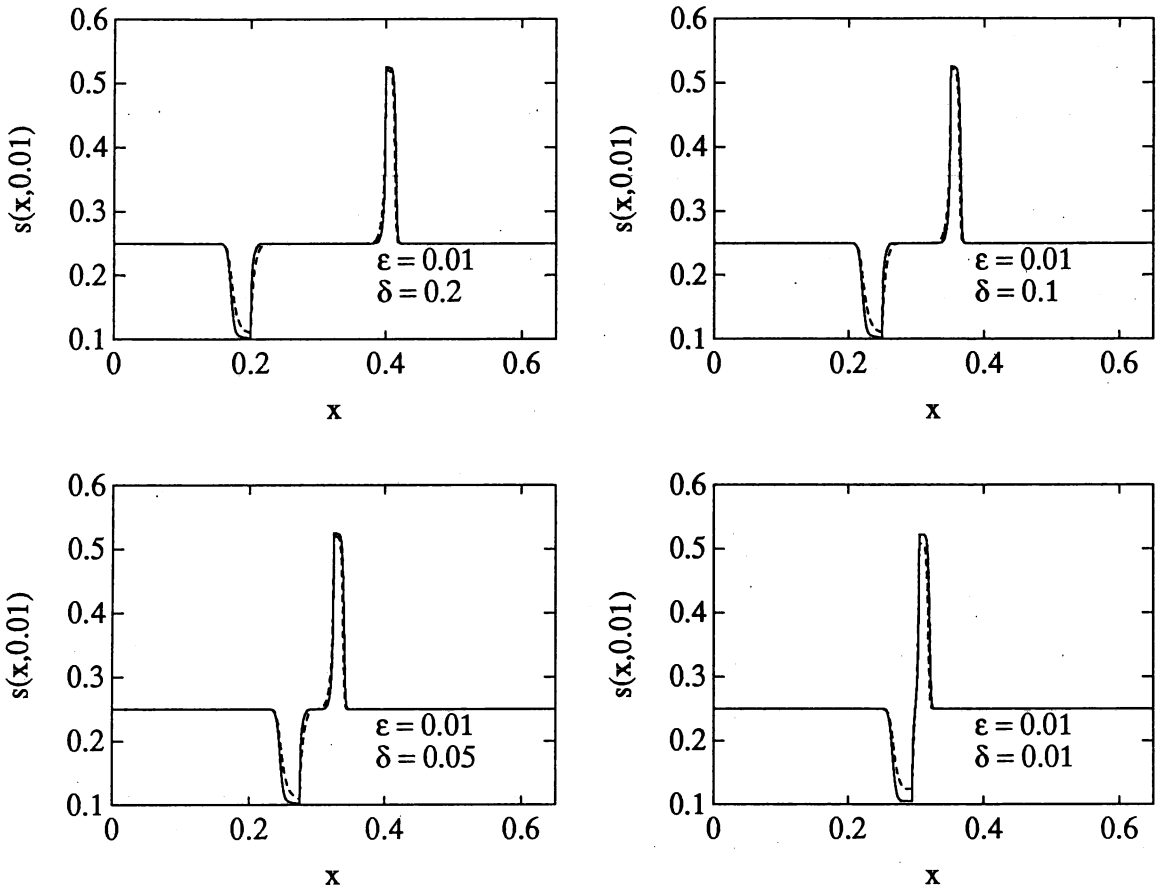

Figure 6: *The numerical solution of the initial value problem for a fixed $\varepsilon = 0.01$ with four different values of δ. Solid line: non-linear diffusion, dotted line: linear diffusion.*

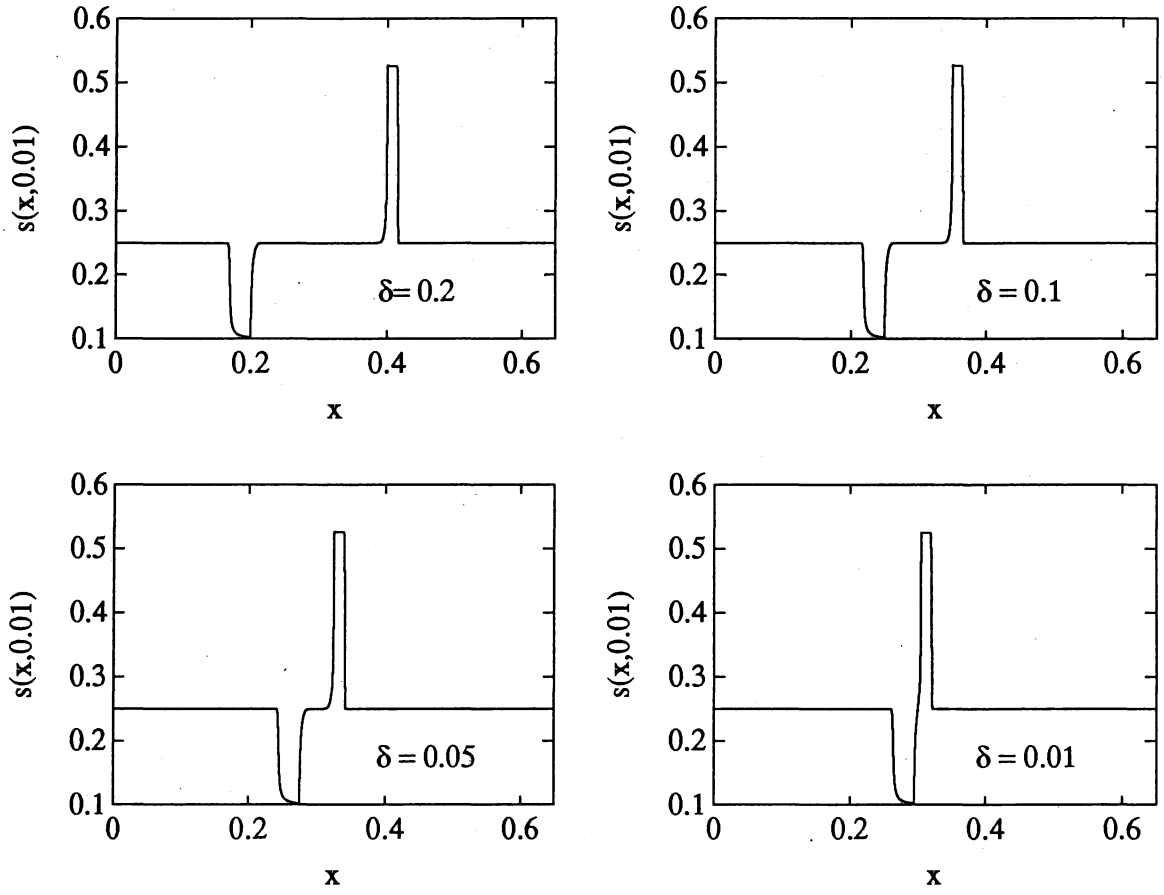

Figure 7: *The numerical solution of the initial value problem for the hyperbolic problem, i.e. for* $\varepsilon = 0$, *with four different values of* δ.

5 A discussion of viscous profiles

The purpose of this section is to give a theoretical discussion of the models (8) and (9) motivated from the experiments above. We will discuss the entropy conditions for the shock waves of (9) and the properties of the associated viscous profiles. In particular, we analyze the shock waves which coincide with a discontinuity in the fractional flow function.

Since the qualitative properties of these models are independent of the values of the positive constants ϕ and v, these parameters are taken to be one throughout this section. Furthermore, since the experiments above indicate that the nonlinearity of the diffusion coefficient ψ has minor influence on the properties of the solutions of the parabolic equation (8), we have also chosen $\psi \equiv 1$. Hence, in this section we shall discuss the relations between the parabolic equation

$$\frac{\partial s}{\partial t} + \frac{\partial f}{\partial x} = \varepsilon \frac{\partial^2 s}{\partial x^2}, \quad \varepsilon > 0, \tag{13}$$

and the hyperbolic equation

$$\frac{\partial s}{\partial t} + \frac{\partial f}{\partial x} = 0 \tag{14}$$

when $f = f(s, x)$ is possibly discontinuous as a function of x at a finite number of spatial points.

Let us first consider possible discontinuous solutions of the hyperbolic equation (14). Assume that $s(x,t)$ is a piecewise smooth solution of (14) which has an isolated discontinuity along a curve $x = \bar{x}(t)$. Then we define

$$s^L = s^L(t) = \lim_{x \to \bar{x}-} s(x,t)$$

and

$$s^R = s^R(t) = \lim_{x \to \bar{x}+} s(x,t).$$

From material balance considerations, or more formally from the requirement that s is a weak solution of (14), we obtain the shock relation

$$f(s^R, \bar{x}+) - f(s^L, \bar{x}-) = \sigma(s^R - s^L), \tag{15}$$

where σ is the shock speed given by $\sigma = d\bar{x}/dt$. If $\sigma \neq 0$, the shock does not follow a discontinuity of the medium. Hence, in this case we can assume that f is continuous

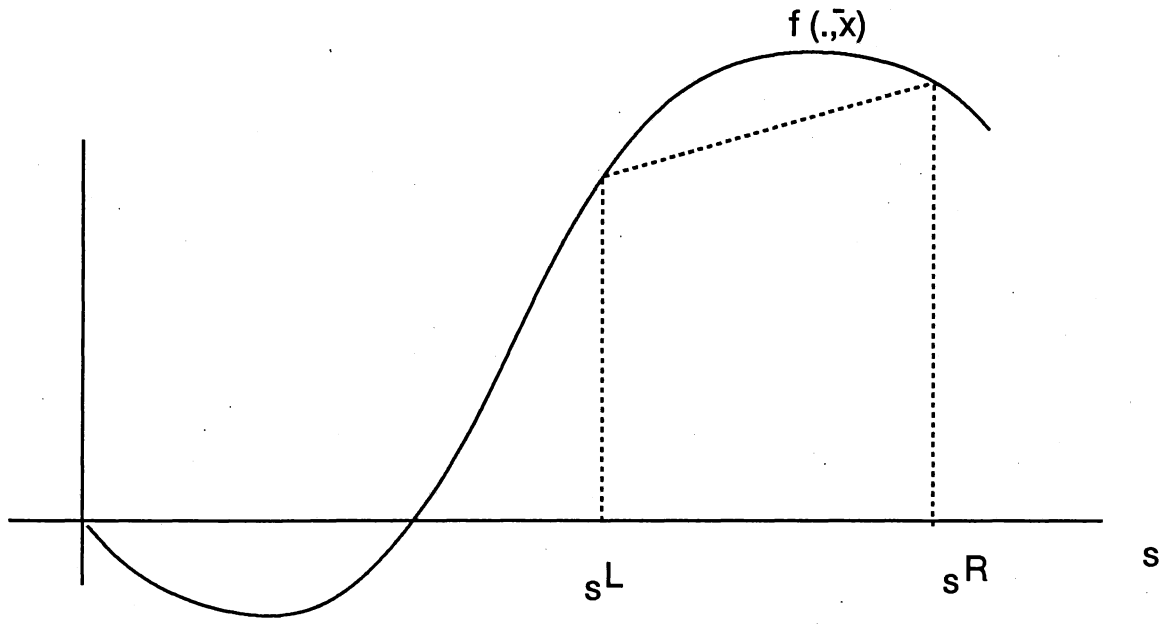

Figure 8: Entropy condition

as function of x at $\bar{x}$. On the other hand, if $\sigma = 0$ the fractional flow function may be discontinuous at $\bar{x}$.

It is well known that in order to obtain unique solutions of hyperbolic conservation laws, all discontinuities satisfying (15) can not be allowed. In addition to the shock condition (15) an entropy condition is required in order to pick the correct physical solution. If $\sigma \neq 0$, and f is continuous at $\bar{x}$, we can adopt the standard entropy condition for scalar conservation laws with a smooth fractional flow function (cf. Lax, 1973, Kruzkov, 1970, or Smoller, 1982). Hence, a discontinuity with $\sigma \neq 0$ satisfying (15) is a proper entropy solution of (14) if (cf. Figure 8)

$$\text{sign}(s^R - s^L)(f(s,\bar{x}) - f(s^L,\bar{x}) - \sigma(s - s^L)) \geq 0. \tag{16}$$

A common approach to derive the entropy condition (16) is from a so-called travelling wave analysis (cf. e.g. Smoller, 1982). Below we will give a similar analysis when $\sigma = 0$ and f is discontinuous at $\bar{x}$. We let $f^-(s) = f(s,\bar{x}-)$ and $f^+(s) = f(s,\bar{x}+)$. Hence, the shock relation takes the form

$$f^-(s^L) = f^+(s^R). \tag{17}$$

The additional entropy condition will be derived from the parabolic equation (13). Locally

around $\bar{x}$ we assume that $f(s,x)$ can be approximated by $\tilde{f}(s,x)$, where

$$\tilde{f}(s,x) = \begin{cases} f^-(s) & \text{if } x < \bar{x}, \\ f^+(s) & \text{if } x > \bar{x}. \end{cases}$$

Furthermore, since we are considering stationary shocks, the equation (13) is replaced by the stationary equation

$$\frac{\partial \tilde{f}}{\partial x} = \varepsilon \frac{\partial^2 s}{\partial x^2}. \tag{18}$$

A piecewise smooth solution $s(x)$ of (18) is, in particular, required to satisfy the continuity condition

$$s(\bar{x}-) = s(\bar{x}+) = \bar{s} \tag{19}$$

and the flux condition

$$f^-(\bar{s}) - \varepsilon \frac{\partial s}{\partial x}(\bar{x}-) = f^+(\bar{s}) - \varepsilon \frac{\partial s}{\partial x}(\bar{x}+). \tag{20}$$

Here the second condition (20) expresses the conservation of mass.

A discontinuity s^L, s^R, satisfying (17), is said to satisfy the entropy condition if it admits a viscous profile, that is, there exists a corresponding similarity solution of (18). A similarity solution $s(x;\varepsilon)$ of (18) corresponding to s^L, s^R is a family of solutions of the form

$$s(x;\varepsilon) = S(\frac{x-\bar{x}}{\varepsilon}),$$

where $S(\zeta)$ satisfies

$$\lim_{\zeta \to -\infty} S(\zeta) = s^L \quad \text{and} \quad \lim_{\zeta \to \infty} S(\zeta) = s^R. \tag{21}$$

Moreover, since s is a solution of (18) we derive, by integrating once with respect to ζ, that S must satisfy the first order equation

$$\frac{dS}{d\zeta} = \tilde{f}(S) - f^-(s^L). \tag{22}$$

The integration constant $f^-(s^L)$, which is equal to $f^+(s^R)$ by (17), follows from (21).

We allow three types of viscous profiles, referred to as a *left profile*, a *right profile* and a *centered profile*. A left profile is a similarity solution of (18) where $S(\zeta) \equiv s^R$ for $\zeta > 0$, that is,

$$s(x;\varepsilon) = \begin{cases} S(\frac{x-\bar{x}}{\varepsilon}) & \text{if } x < \bar{x}, \\ s^R & \text{if } x > \bar{x}, \end{cases}$$

where $S(-\infty) = s^L$. Furthermore, (19) implies that $S(0) = s^R$, while condition (20) is automatically satisfied by (17). Hence, the discontinuity s^L, s^R admits a left profile if and only if there exist a solution $S(\zeta)$ of (22) such that

$$S(-\infty) = s^L \quad \text{and} \quad S(0) = s^R.$$

A necessary and sufficient condition to guarantee this is that

$$\text{sign}(s^R - s^L)(f^-(s) - f^-(s^L)) > 0$$

for all s between s^L and s^R. In consistency with the entropy condition (16) for scalar conservation laws with a smooth flux function we also allow discontinuities which admits a composition of several left profiles. Hence, a discontinuity s^L, s^R, satisfying (17), is an entropy shock with a left viscous profile if

$$\text{sign}(s^R - s^L)(f^-(s) - f^-(s^L)) \geq 0 \tag{23}$$

for all s between s^L and s^R.

By similar arguments as given above we can also derive conditions which guarantee the existence of solutions of (18) of the form

$$s(x;\varepsilon) = \begin{cases} s^L & \text{if } x < \bar{x}, \\ S(\frac{x-\bar{x}}{\varepsilon}) & \text{if } x > \bar{x}, \end{cases}$$

and conclude that the entropy condition with a right viscous profile is satisfied if

$$\text{sign}(s^R - s^L)(f^+(s) - f^+(s^R)) \geq 0 \tag{24}$$

for all s between s^L and s^R. The conditions (23) and (24) are illustrated in Figure 9, and typical left and right profiles are depicted in Figures 10 and 11, respectively.

Finally, a centered profile is a similarity solution $s(x;\varepsilon) = S(\frac{x-\bar{x}}{\varepsilon})$ of (18) which is neither a left profile nor a right profile. By arguments similar to those given above we derive that a discontinuity s^L, s^R, satisfying (17), is an entropy shock with a centered viscous profile if there exists an $\bar{s}$ such that

$$\begin{aligned} &i) \quad \text{for all } s \text{ between } s^L \text{ and } \bar{s} \\ &\qquad \text{sign}(\bar{s} - s^L)(f^-(s) - f^-(s^L)) \geq 0, \\ &ii) \quad \text{for all } s \text{ between } \bar{s} \text{ and } s^R \\ &\qquad \text{sign}(s^R - s^L)(f^+(s) - f^+(s^R)) \geq 0. \end{aligned} \tag{25}$$

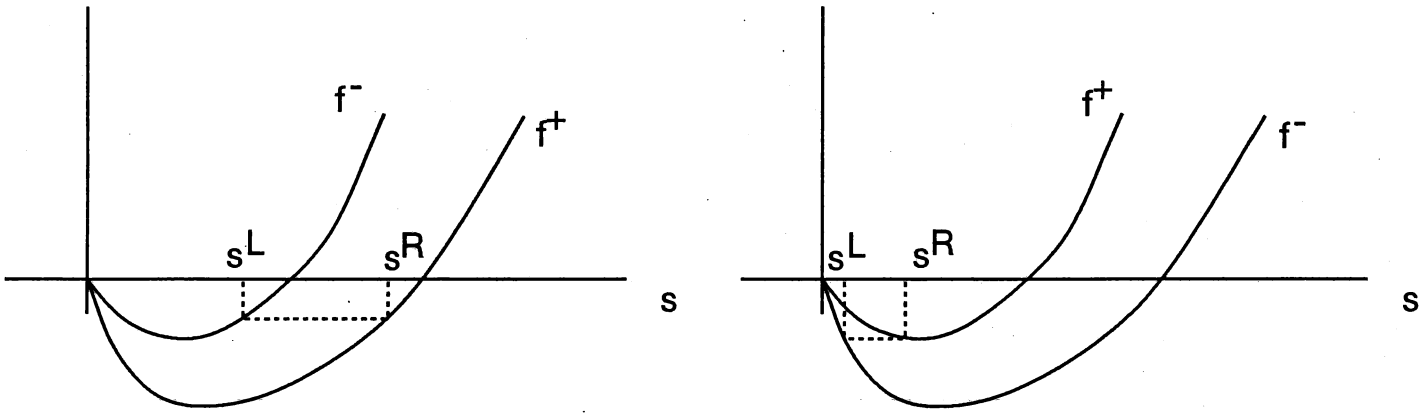

Figure 9: *Entropy conditions corresponding to left and right profiles*

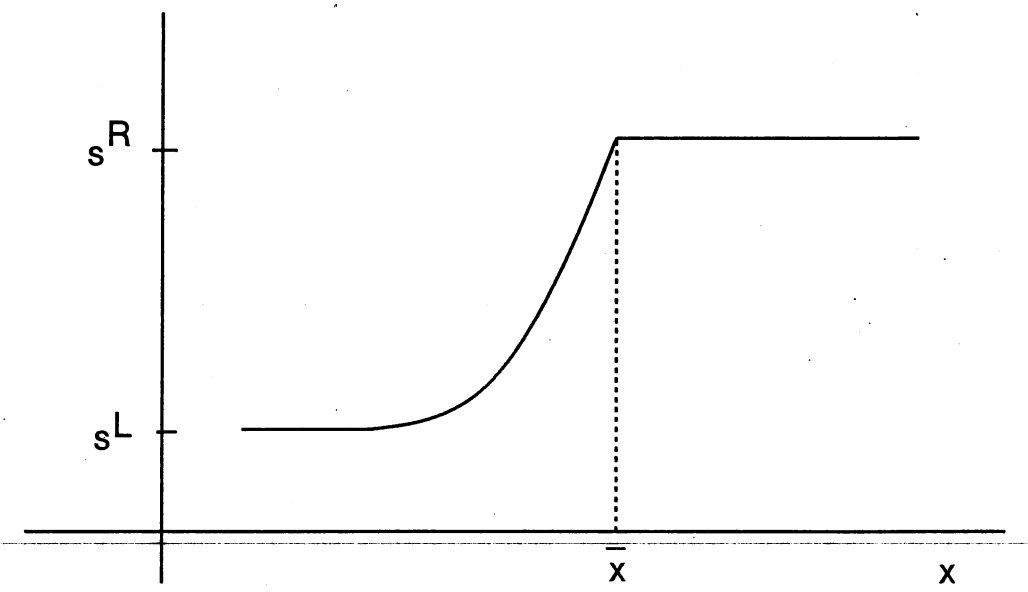

Figure 10: *Left profile.*

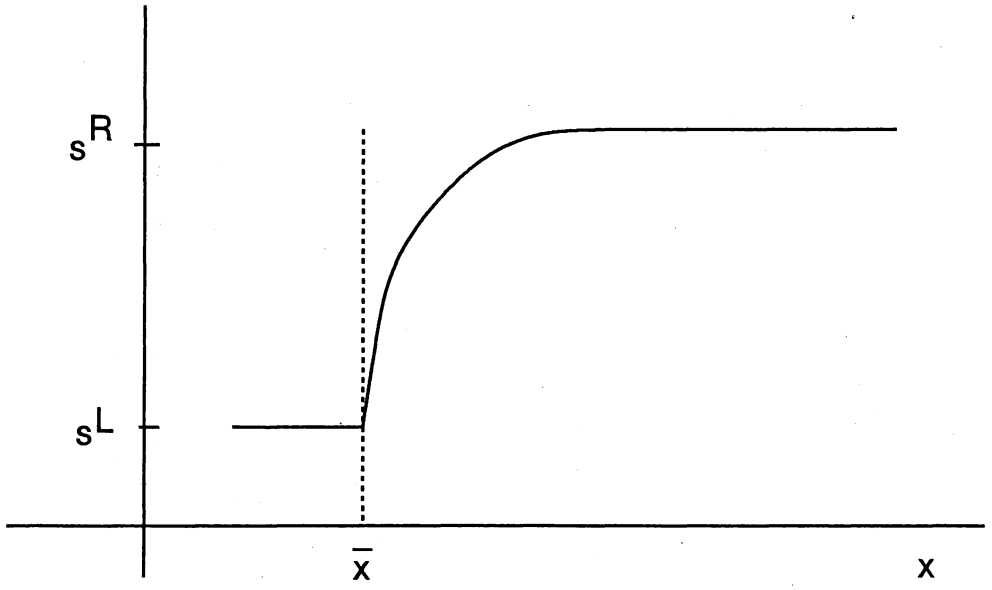

Figure 11: *Right profile.*

The condition (25) is illustrated in Figure 12 and a typical centered profile is depicted in Figure 13.

In summary we conclude that a discontinuity s^L, s^R, satisfying (17), is said to be an entropy shock at $\bar{x}$ if one of the three conditions (23)–(25) holds.

We will use the viscous profiles derived above in order to discuss the results of Sections 4 and 5. Recall the initial value problem for the hyperbolic equation studied in Section 3 which consists of two noninteracting Riemann problems. The solution of this problem is composed of four shocks as illustrated by Figures 1 and 2. The slow shock of the left Riemann problem and the fast shock of the right Riemann problem are ordinary scalar shocks corresponding to a continuous fractional flow function, while the two intermediate shocks correspond to a discontinuous fractional flow function as described above. In particular, both these intermediate shocks have speed zero, and therefore the initial distance between them, δ, remains the same for all time.

If we consider the two intermediate shocks in view of the discussion of viscous profiles above, we easily discover that they both satisfy the entropy condition. Furthermore, the shock of the left Riemann problem has a right profile, while the shock of the right Riemann problem has a left profile. Hence, this indicates, that when δ is sufficiently large compared

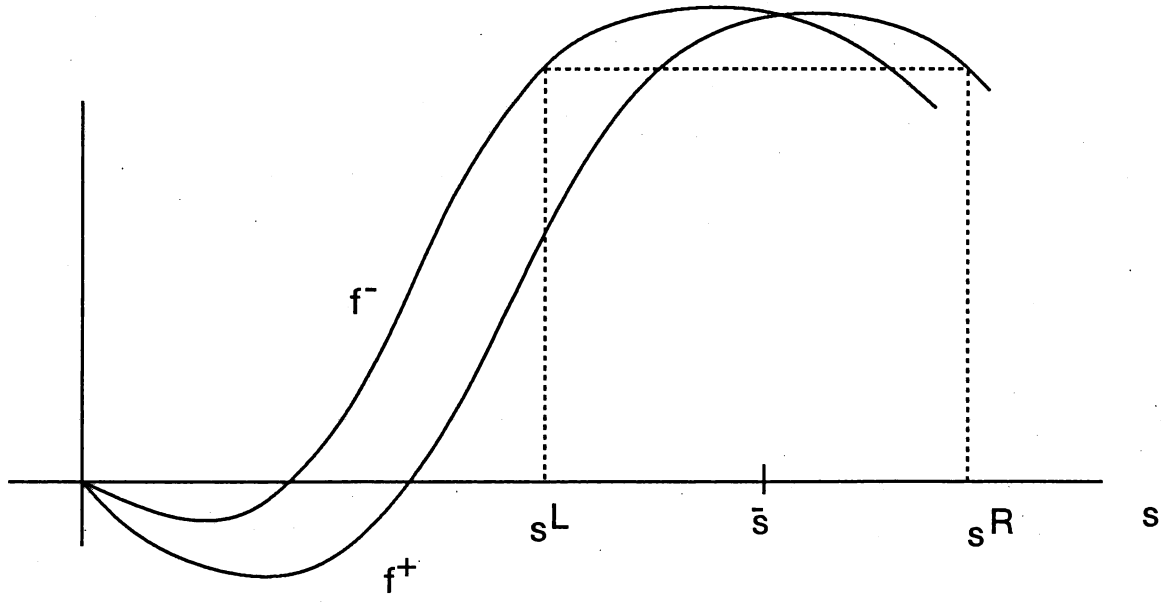

Figure 12: Entropy condition corresponding to a centered profile

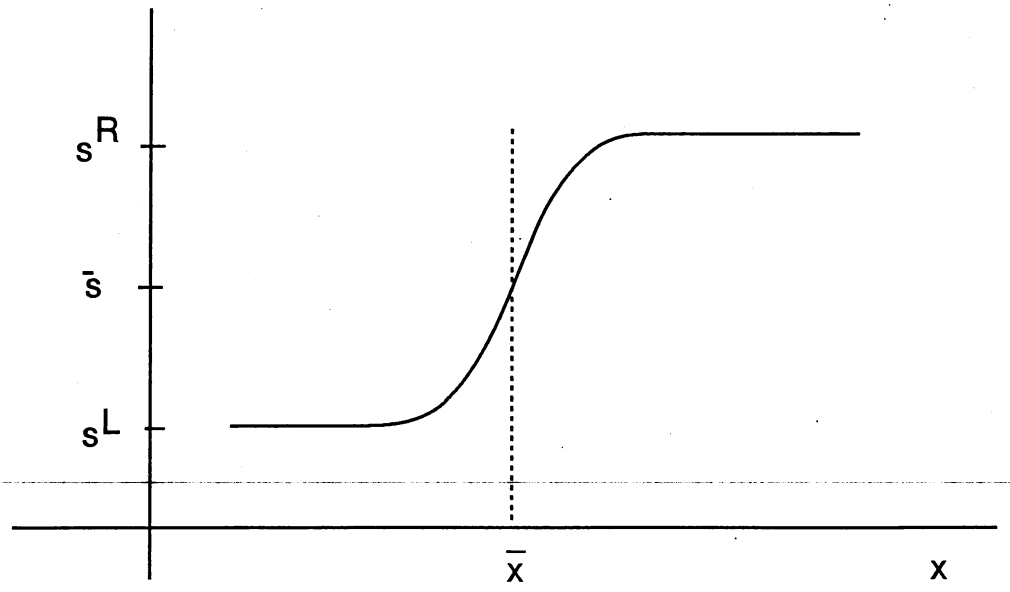

Figure 13: *Centered profile.*

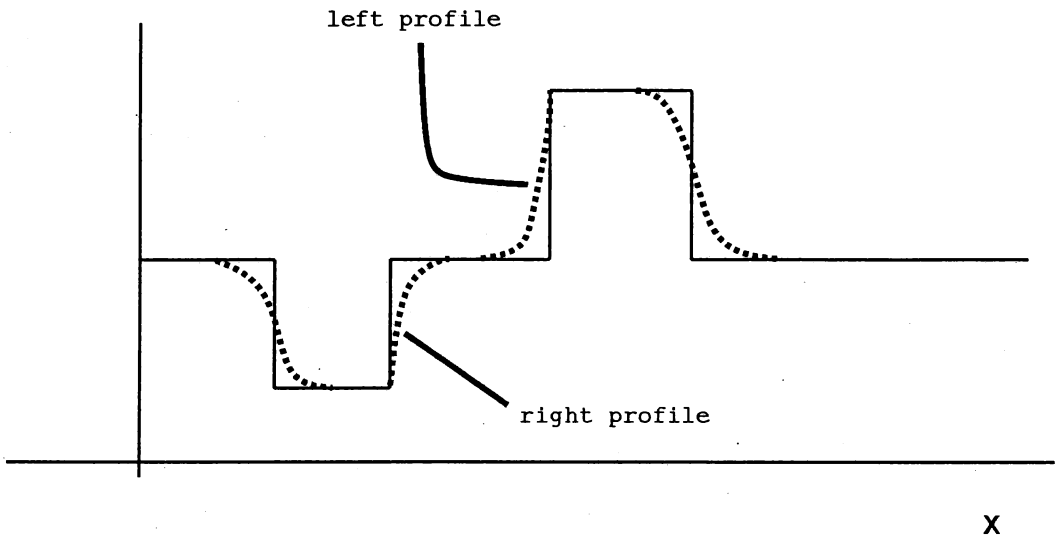

Figure 14: *The solution of the hyperbolic problem is drawn with a solid, and the solution of the parabolic problem is drawn with a dotted line.*

to ε, the solution of the hyperbolic equation and the corresponding solution of the parabolic equation have the forms sketched in Figure 14, where the profiles decays to S_1 as a function of $1/\varepsilon$ times the distance to the shock.

However, when δ becomes sufficiently small compared to ε, the two viscous profiles for the intermediate waves will interact. This therefore partially explains the observation done in Section 4 that the parabolic solution and the hyperbolic solution behave qualitatively different when δ is small.

6 Conclusions

In this paper we have studied the Buckley–Leverett equation modelling one–dimensional, incompressible two–phase flow in a heterogeneous porous medium with gravity effects. The heterogeneity corresponded to a layered reservoir with a thin internal low permeable region. It has been shown both by analytical solutions and by numerical experiments that the hyperbolic version of this model is unstable in the sense that perturbations in physical parameters in a tiny region of the reservoir may lead to a totally different flow picture. A

consequence is that simulation results obtained by solving the hyperbolic Buckley–Leverett equation are unreliable. We have also studied diffusion effects in the flow model. Roughly speaking, the stability decreases with decreasing diffusion. Our main limitation of the one–dimensional flow model used herein is considered to be the assumption of uni–directional flow. However, in two– and three–dimensional flow situations the instability phenomenon is expected to arise if the flow is locally uni–directional and if the internal low permeable layer has a sufficiently large extent in the directions normal to the flow.

It must be emphasized that all our results concern the mathematical model. Physical experiments are required to determine whether the instability effects have any physical significance. Similar instability phenomenon are obviously present in other mathematical models consisting of hyperbolic partial differential equations, for example the equations governing sound or water surface waves in heterogeneous media.

References

[1] Allen III, M. B., Behie, G. A. and Trangenstein, J. A., 1988, Multiphase flow in porous media. *Lecture notes in engineering, Springer-Verlag.*

[2] Aziz and Settari, 1979, Petroleum reservoir simulation. *Applied Science Publishers, London.*

[3] Gimse, T. and Risebro, N. H., 1990, Riemann problems with a discontinuous flux function, Presented at the third international conference on hyperbolic problems in Uppsala.

[4] Isaacson, E. and Temple, B., The structure of asymptotic states in a singular system of conservation laws, preprint.

[5] Kruzkov, S. N., 1970 First order quasilinear sequations with several space variables, Math. USSR. Sb. 10 , pp. 217-243.

[6] Lax, P.D., 1973, Hyperbolic systems of conservation laws and the mathematical theory of shock waves, Conf. Board Math. Sci., 11, SIAM.

[7] Lucier, B., 1985, Error bounds for the methods of Glimm, Godunov and LeVeque, Siam J. Num. Anal. **22** pp. 1074-1081.

[8] Smoller, J., 1982, Shock waves and reaction-diffusion equations, *Springer Verlag, New York.*

[9] Tveito, A. and Winther, R., 1990, A well posed system of hyperbolic conservation laws, Presented at the third international conference on hyperbolic problems in Uppsala.